Research Square

Preprints are preliminary reports that have not undergone peer review.
They should not be considered conclusive, used to inform clinical practice,
or referenced by the media as validated information.

Broadleaf companion species shape ecosystem carbon storage in underplanted Pinus massoniana plantations

Zeyao Zhao
Huazhong Agricultural University
Nan Jiang
Huazhong Agricultural University
Wenjun Xie
Huazhong Agricultural University
Kangwei Zhao
Huazhong Agricultural University
Jieyu Zhang
Huazhong Agricultural University
Miaoyan Quan
Huazhong Agricultural University
Zhaogui Yan
Huazhong Agricultural University
Li Mei
meili@mail.hzau.edu.cn

Huazhong Agricultural University

Research Article

Keywords: Broadleaf underplanting, Companion species identity, Ecosystem carbon stocks, Mineral-associated organic carbon, Microbial biomass carbon, Soil depth

Posted Date: November 23rd, 2026

DOI: https://doi.org/10.21203/rs.3.rs-11465704/v1

License: This work is licensed under a Creative Commons Attribution 4.0 International License.
Read Full License

Additional Declarations: No competing interests reported.

Broadleaf companion species shape ecosystem carbon storage in underplanted *Pinus massoniana* plantations

Zeyao Zhao[a], Nan Jiang[a], Wenjun Xie[a], Kangwei Zhao[a], Jieyu Zhang[a], Miaoyan Quan[a], Zhaogui Yan[a], Li Mei[a, *]

[a] College of Horticulture and Forestry Sciences/Hubei Engineering Technology Research Center for Forestry Information, Huazhong Agricultural University, Wuhan 430070, China

* Email of the corresponding author: meili@mail.hzau.edu.cn

Abstract

Broadleaf underplanting can increase forest carbon (C) storage, but whether companion species differ in their contributions to tree and soil C stocks remains unclear. We compared pure *Pinus massoniana* stands (*PM*) with stands underplanted with *Osmanthus fragrans* (*PO*) or *Schima superba* (*PS*) 11 years earlier in subtropical China. We quantified vegetation and litter C stocks, soil C stocks to 60 cm on an equivalent soil mass basis, and soil nutrients, microbial biomass, potential enzyme activities, and topsoil fungal communities. Ecosystem C stocks were 50.8% higher in *PO* and 68.5% higher in *PS* than in *PM*. Retained pines accounted for most of the higher live tree C in both mixtures relative to *PM*. Compared with *PO*, *PS* stored 11.8% more ecosystem C, 12.5% more soil organic carbon (SOC), and 4.8 times as much C in broadleaf trees, despite lower litter C. *P. massoniana* and total live tree C stocks did not differ significantly between the mixtures. Mineral-associated organic carbon (MAOC) accounted for over 96% of the SOC stock differences between each mixture and *PM*, while particulate organic carbon (POC) stocks did not differ significantly among treatments. MAOC concentrations were higher throughout the sampled profile, with the largest proportional differences at 40–60 cm. After accounting for treatment and soil layer, microbial biomass C was more strongly associated with MAOC than with POC. These results favor *S. superba* over *O. fragrans* for ecosystem C storage at this site, with its advantage reflected in broadleaf tree C and MAOC.

Keywords: Broadleaf underplanting; Companion species identity; Ecosystem

carbon stocks; Mineral-associated organic carbon; Microbial biomass carbon; Soil depth

1 Introduction

Forests remain a major terrestrial carbon (C) sink, with living biomass and soils containing most forest C (Pan et al., 2024). Managing plantations for C storage therefore requires considering both tree and soil C pools. Broadleaf underplanting introduces companion trees beneath an existing conifer canopy, allowing managers to diversify established plantations while retaining canopy trees. Multispecies plantations generally outyield monocultures across contrasting environments, while greater tree diversity promotes soil carbon accrual over decadal timescales (Feng et al., 2022; Chen et al., 2023). These benefits vary with species composition and environmental conditions. Mycorrhizal associations modify diversity–productivity relationships, resource use strategies alter productivity responses to mixing, and canopy structural complexity strengthens complementarity among tree species (Luo et al., 2024; Jensen et al., 2025; Deng et al., 2025). Recent work also links functional diversity and environmental variation to ecosystem carbon storage in subtropical forests (Wu et al., 2025). For underplanting decisions, a central question is how companion species differ in ecosystem C stocks and in the contributions of retained trees, companion trees, and soil.

Companion trees contribute to ecosystem C storage through their own biomass, their interactions with retained trees, and their inputs to soil. Species differ in growth and resource acquisition strategies, litter chemistry, rooting patterns, and associations with soil biota. These differences influence stand productivity as well as the quantity and quality of carbon entering soil (Augusto and Boča, 2022; Jensen et al., 2025). For

example, introducing broadleaf trees into a conifer plantation increased stand resource use efficiency and gross primary productivity, even though competition constrained conifer growth (Liu et al., 2024). Belowground, neighbor identity alters root exudation and rhizosphere bacterial communities (Ulbrich et al., 2022). In *Pinus massoniana* plantations, mixing with a broadleaf tree species altered litter and fine root C chemistry and soil organic carbon (SOC) composition, with fine root traits more closely associated with SOC composition than litter traits (Wang et al., 2019). More recent studies connect *P. massoniana* mixture composition with soil nutrient status and SOC stocks across contrasting restoration contexts (Yang et al., 2025; Tang et al., 2025). Experiments have also shown that tree diversity can affect aboveground and belowground C pools differently (Schnabel et al., 2025). Whether retained-tree and soil C stocks vary in parallel among companion species in underplanted pine stands remains unclear.

Evaluating soil C storage also requires identifying the fractions and depths in which C stocks differ. Particulate organic carbon (POC) consists largely of partially decomposed plant residues and remains closely linked to litter and root inputs. Mineral-associated organic carbon (MAOC) includes organic compounds associated with mineral surfaces, including products of microbial transformation, and often persists longer than POC (Lavallee et al., 2020; Sokol et al., 2022). A recent global synthesis found that mixed forestation increased SOC, POC, and MAOC, with MAOC more closely associated with SOC gains than POC (Shu et al., 2026). Research in *P. massoniana* forests also links soil C retention in conifer and broadleaf

mixtures to aggregation and associations with Fe oxides (Han et al., 2024). The relative contributions of POC and MAOC may also vary with depth as plant inputs, microbial activity, and mineral conditions change down the profile. SOC fractions vary markedly with depth in subtropical *P. massoniana* forests (Yuan et al., 2022), and forestation effects on these fractions differ among soil layers (Shu et al., 2026). In pine stands with broadleaf underplanting, the relative contributions of POC and MAOC to SOC stock differences across soil depths remain poorly characterized.

Soil nutrient availability and microbial processes may help explain differences in SOC fractions among companion species. Tree species mixing alters microbial biomass, community composition, and enzyme activities in subtropical plantations (Huang et al., 2014, 2017). Vegetation also influences genes involved in C degradation and microbial metabolic activity, with associated changes in SOC pools (Huang et al., 2024). Extracellular enzymes break down organic substrates and release compounds that microorganisms can use for growth. Microbial growth and turnover generate products that can contribute to MAOC formation (Sokol et al., 2022). Microbial biomass may therefore be more closely associated with MAOC than with POC. Examining the relationships of both C fractions with microbial biomass, nutrient availability, and enzyme activities can help interpret differences in soil C storage among companion species.

Here, we compared carbon storage among pure *Pinus massoniana* plantations and plantations underplanted 11 years earlier with either *Osmanthus fragrans* or *Schima superba*. We quantified C stocks in *P. massoniana*, companion trees, understory

vegetation, litter, and soil to identify the pools accounting for differences in ecosystem C storage. We compared POC and MAOC across the 0–60 cm soil profile and measured soil nutrient availability, microbial biomass, and potential enzyme activities. We also characterized topsoil fungal community composition and bacterial and fungal alpha diversity. We tested three hypotheses: (i) underplanted stands would store more ecosystem C than pure *P. massoniana* stands, with companion species differing in the contributions of retained pines, companion trees, and soil to ecosystem C stocks; (ii) higher SOC stocks in underplanted stands would chiefly reflect greater MAOC stocks, with differences extending into deeper soil layers; and (iii) microbial biomass C would be more strongly associated with MAOC than with POC.

2 Materials and methods

2.1 Study site

This study was conducted in Sanming, Fujian Province, southeastern China (26°21′ N, 117°11′ E). The region has a humid subtropical monsoon climate, with a mean annual temperature of 19.1 °C and mean annual precipitation of approximately 1750 mm. Low mountains and hills dominate the landscape. Soils are classified as Oxisols under USDA Soil Taxonomy (Jia et al., 2024). The zonal vegetation is subtropical evergreen broadleaved forest. Common understory species included *Woodwardia japonica*, *Rubus corchorifolius*, *Ardisia kwangtungensis*, and *Dicranopteris pedata*.

2.2 Experimental design and stand inventory

A *Pinus massoniana* plantation was established in 1992 at an initial density of 3,000 stems ha^{-1}. In April 2002, the plantation was thinned by approximately 85% to 450

stems ha^{-1}. In 2013, two-year-old seedlings of *Osmanthus fragrans* and *Schima superba* were underplanted separately, each at 450 stems ha^{-1}. The study compared three planting treatments: pure *P. massoniana* (*PM*), *P. massoniana* mixed with *O. fragrans* (*PO*), and *P. massoniana* mixed with *S. superba* (*PS*). Three independent stands were selected for each planting treatment, and one 20 × 20 m plot was randomly established within each stand, yielding nine plots. All plots were located on southwest-facing slopes of 19–20°. Plots were at least 200 m apart.

Field sampling was conducted in November 2024, 11 years after broadleaf underplanting. All live trees within each plot were identified to species. Diameter at breast height (DBH) was measured at 1.3 m above ground to the nearest 0.1 cm using a diameter tape. Tree height was measured with a hypsometer.

2.3 Plant and litter sampling and carbon stock estimation

For each tree species in each plot, five trees with DBH and height close to the corresponding species means were selected for tissue sampling. Healthy leaves and current year branches were collected from the upper middle crown in four cardinal directions. Stem wood was sampled after removing the bark. Fine roots (<2 mm in diameter) were collected along four radial transects around each selected tree. Three 2 × 2 m subplots were established in each plot for understory sampling. All understory vegetation within each subplot was harvested and separated into aboveground and belowground components. Forest floor litter was collected from three 1 × 1 m quadrats in each plot.

Plant and litter samples were oven-dried at 65 °C to constant mass and weighed.

Dried samples were ground to pass through an 80-mesh sieve. Carbon concentration was then determined by potassium dichromate oxidation (Bao, 2000). Biomass of stems, branches, leaves, and roots was estimated for each inventoried tree from DBH using allometric equations (Luo et al., 2020; Table S1). Individual tree estimates were summed within each plot. Understory and litter biomass were calculated from dry mass and sampled area. Carbon stock for each component was calculated by multiplying its biomass by the corresponding measured carbon concentration. Live tree C stock was calculated by summing component C stocks across all trees within each plot.

2.4 Soil sampling, physicochemical analyses, and carbon fractionation

After removing the surface litter, five sampling points were randomly selected within each plot. Mineral soil was collected at 0–20 cm (topsoil), 20–40 cm (midsoil), and 40–60 cm (subsoil). Samples from the five points were combined and homogenized by depth within each plot to form one composite sample. Three intact soil cores were also collected at each depth in each plot using 6-cm diameter stainless steel rings. Composite samples were transported to the laboratory on ice. Visible roots, stones, and plant residues were removed, and the soil was passed through a 2-mm sieve. After sieving, one fresh portion was stored at 4 °C for inorganic N, microbial biomass, and enzyme assays. A second portion was air-dried for soil chemical analyses and organic carbon fractionation. For topsoil samples, a third portion was stored at −80 °C for bacterial and fungal community analyses.

Soil water content, bulk density, total porosity, capillary porosity, and non-capillary

porosity were determined from the intact cores by the ring-core method (Qi et al., 2022). The cores were oven-dried at 105 °C to constant mass, and bulk density was calculated from dry soil mass and core volume. Measurements from the three cores were averaged for each plot and depth.

Soil pH was measured in a 1:2.5 soil-to-water suspension. Soil organic carbon (SOC) was determined by potassium dichromate oxidation, and total nitrogen (TN) was determined by Kjeldahl digestion. Total phosphorus (TP) was determined by molybdenum blue colorimetry after acid digestion. Alkali-hydrolysable N (AN) was determined by alkaline hydrolysis diffusion. Available P (AP) was extracted with Bray-1 solution and determined by molybdenum blue colorimetry (Bao, 2000). For inorganic N, 20 g of fresh soil was extracted with 100 mL of 2 mol L^{-1} KCl for 1 h. After filtration, NH_4^+-N and NO_3^--N were determined by the indophenol blue and cadmium reduction methods, respectively.

Particulate organic carbon (POC) was separated by particle-size fractionation (Sokol and Bradford, 2019; Huang et al., 2024). A 20-g subsample of air-dried soil was dispersed in 60 mL of 5 g L^{-1} sodium hexametaphosphate for 18 h. The suspension was then wet sieved through a 53-μm sieve. The retained fraction (>53 μm) was dried at 65 °C, weighed, ground, and analyzed for organic carbon. POC concentration was calculated from the dry mass and carbon concentration of the retained fraction. Mineral-associated organic carbon (MAOC) was calculated as SOC minus POC.

2.5 Soil and ecosystem carbon stock estimation

For each soil layer, SOC, POC, and MAOC stocks were calculated from carbon

concentration, bulk density, and layer thickness. Layer-specific stocks were summed to obtain fixed depth stocks for the 0–60 cm profile. SOC, POC, and MAOC stocks were also expressed on an equivalent soil mass (ESM) basis (Wendt and Hauser, 2013). The smallest cumulative soil mass to 60 cm among the nine plots was used as the common reference mass. For plots with greater soil mass, only the required proportion of the 40–60 cm layer was included to match the reference mass. ESM stocks were used in the main analyses, whereas fixed depth stocks were retained for comparison. Total ecosystem C stock was calculated as the sum of live tree, understory, litter, and 0–60 cm ESM SOC stocks.

2.6 Soil microbial biomass and potential enzyme activities

Microbial biomass carbon (MBC), nitrogen (MBN), and phosphorus (MBP) were measured in fresh soil by chloroform fumigation–extraction (Joshi and Garkoti, 2023; Yu et al., 2024). Paired subsamples were fumigated with ethanol free $CHCl_3$ for 24 h or left unfumigated. MBC and MBN were extracted with 0.5 mol L^{-1} K_2SO_4, whereas MBP was extracted with 0.5 mol L^{-1} $NaHCO_3$ at pH 8.5. Microbial biomass was calculated from differences between fumigated and unfumigated extracts using extraction coefficients of 0.45, 0.54, and 0.40 for MBC, MBN, and MBP, respectively. The potential activities of β-1,4-glucosidase (BG), β-1,4-N-acetylglucosaminidase (NAG), acid phosphatase (ACP), and peroxidase (PER) were measured using substrate-specific microplate assays (Qi et al., 2022; Huang et al., 2024). Fresh soil (1.5 g) was suspended in 100 mL of sodium acetate buffer (50 mmol L^{-1}, pH 4.5). The slurry was vortexed for 1 min and stirred for 1 h. BG, NAG, and ACP were assayed

using p-nitrophenyl-β-D-glucopyranoside, 4-methylumbelliferyl-N-acetyl-β-D-glucosaminide, and disodium phenyl phosphate, respectively. PER was assayed using L-3,4-dihydroxyphenylalanine with H_2O_2 as the oxidant. Reactions were incubated in darkness at 20 °C for 4 h. BG, NAG, and ACP activities were expressed as nmol g^{-1} h^{-1} and PER activity as μmol g^{-1} h^{-1}, all on an oven-dry soil basis.

2.7 Amplicon sequencing and sequence processing

Bacterial and fungal communities were characterized in composite topsoil samples (0–20 cm) from each plot. Total genomic DNA was extracted from each sample using the TGuide S96 Magnetic Soil/Stool DNA Kit. The V3–V4 region of the bacterial 16S rRNA gene and the fungal ITS1 region were amplified. Purified amplicons were sequenced as paired end reads (2 × 250 bp) on an Illumina NovaSeq 6000 platform. Raw reads were quality filtered and merged, and ASVs were generated using DADA2. Taxonomy was assigned in QIIME 2 using SILVA 138.1 for bacteria and UNITE for fungi. Fungal trophic modes were assigned using FUNGuild (Nguyen et al., 2016) and summarized as symbiotrophs, saprotrophs, and pathotrophs. Bacterial and fungal Shannon, Simpson, Chao1, and ACE indices were used to characterize alpha diversity. For fungal community analyses, ASVs occurring in fewer than two samples or represented by fewer than 10 reads across all samples were removed. For descriptive visualization, six ECM fungal genera showing contrasting abundance patterns among treatments were selected.

2.8 Statistical analyses

All statistical analyses were conducted in R version 4.4.1 (R Core Team, 2024).

Unless otherwise stated, data are presented as means ± SE and model estimates with 95% confidence intervals (CIs). Statistical significance was set at $P < 0.05$.

One-way analysis of variance (ANOVA) was used to test planting treatment effects on plot level plant and litter variables, ecosystem C stock, 0–60 cm ESM SOC, POC and MAOC stocks, and bacterial and fungal alpha diversity indices. Tukey adjusted pairwise comparisons were used to compare treatment means. Broadleaf variables were compared between *PO* and *PS* because broadleaf trees were absent from *PM*. Linear mixed-effects models were used to test the effects of planting treatment, soil layer, and their interaction on SOC, POC, and MAOC concentrations and on soil nutrient, microbial biomass, and enzyme variables. Plot was included as a random intercept, and models were fitted by restricted maximum likelihood. For SOC, POC, and MAOC, Tukey-adjusted estimated marginal means were used to compare planting treatments within each soil layer and soil layers within each planting treatment. For soil nutrient, microbial biomass, and enzyme variables, Tukey-adjusted contrasts compared *PO* with *PM*, *PS* with *PM*, and *PS* with *PO* within each soil layer. These variables were natural-log transformed, and model estimates were back transformed to percentage differences as $100[\exp(\beta) - 1]$. A joint mixed-effects model fitted to natural-log-transformed 0–60 cm POC and MAOC stocks was used to compare treatment responses between carbon fractions. Log response ratios (lnRRs) were estimated for *PO* and *PS* relative to *PM*, and differences between MAOC and POC responses were tested using Holm-adjusted contrasts.

Fungal community composition was analyzed using centered-log-ratio-transformed

ASV data and Aitchison distances. Principal coordinates analysis (PCoA) was used to visualize compositional differences among planting treatments, which were tested using exact PERMANOVA. Differences in multivariate dispersion were tested using PERMDISP.

Five separate linear mixed-effects models were used to compare the associations of AN, AP, MBC, BG, and PER with POC and MAOC. Predictors and carbon fractions were natural log transformed and standardized before analysis. Models accounted for planting treatment and soil layer, with plot and plot × soil layer included as random intercepts. Fraction-specific standardized slopes and their MAOC − POC differences were estimated using Kenward–Roger degrees of freedom, and the five slope-difference *P* values were adjusted using the Benjamini–Hochberg procedure.

3 Results

3.1 *PS* stored the most ecosystem C

PO and *PS* stored 50.8% and 68.5% more ecosystem C than *PM*, respectively (173 and 193 vs. 115 Mg C ha^{-1}; both $P < 0.001$; Fig. 1). *PS* stored 11.8% more ecosystem C than *PO* ($P < 0.05$). *PO* and *PS* stored 97.8% and 89.4% more C in *P. massoniana* than *PM*, respectively (71.1 and 68.1 vs. 36.0 Mg C ha^{-1}; Table S2). *PS* and *PO* stored similar amounts of C in *P. massoniana* ($P > 0.05$), whereas *PS* stored 4.8 times as much C in broadleaf trees as *PO* (16.6 vs. 3.5 Mg C ha^{-1}; $P < 0.05$; Table S2-S4). *PS* had a 13.6% higher mean live tree C stock than *PO*, although this difference was not significant (84.7 vs. 74.6 Mg C ha^{-1}; $P > 0.05$). *PS* also stored 12.5% more SOC than *PO* (106 vs. 94.6 Mg C ha^{-1}; $P < 0.001$). Soil was the largest ecosystem C pool in all

three treatments, accounting for 54.8–66.8% of the total (Fig. 1b).

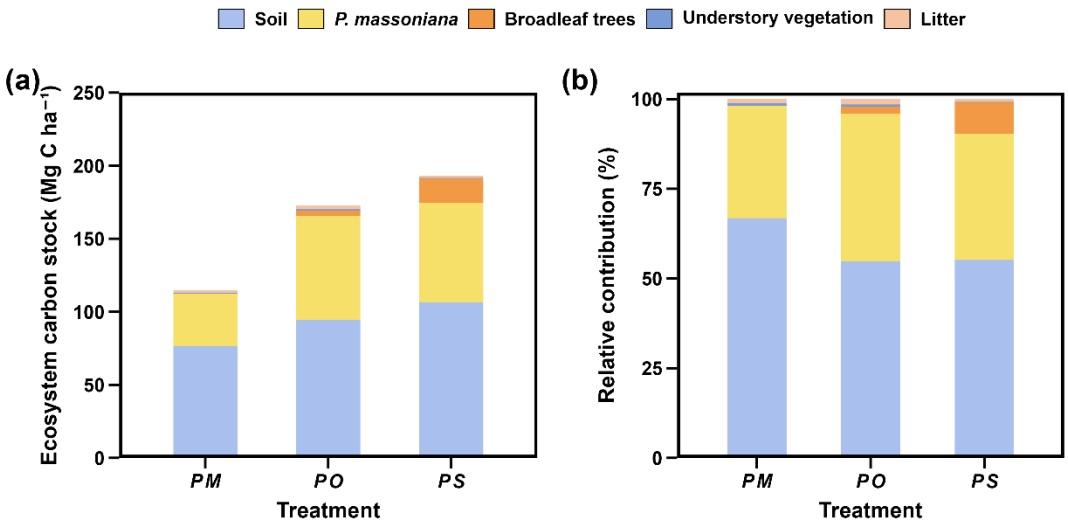

Fig. 1 Carbon stocks and their distribution among ecosystem pools under the three planting treatments. (a) Absolute carbon stocks and (b) relative contributions of soil, *P. massoniana*, broadleaf trees, understory vegetation, and litter to total ecosystem C stocks. *PM*, pure *P. massoniana*; *PO*, *P. massoniana* mixed with *Osmanthus fragrans*; *PS*, *P. massoniana* mixed with *Schima superba*.

3.2 *PO* and *PS* had higher MAOC stocks but similar POC stocks

PO and *PS* had higher SOC and MAOC concentrations than *PM* across all three soil layers, whereas POC concentrations differed little among treatments (Fig. 2). Relative to *PM*, MAOC concentrations were 24.1–67.3% higher in *PO* and 43.9–99.5% higher in *PS*. Both mixtures had their largest proportional differences in MAOC concentration relative to *PM* in the subsoil. Across 0–60 cm, *PO* and *PS* stored 38.1% and 60.9% more MAOC than *PM*, respectively (64.9 and 75.6 vs. 47.0 Mg C ha^{-1}; both $P < 0.05$; Fig. 2d). *PS* stored 16.5% more MAOC than *PO* ($P < 0.05$), whereas POC stocks did not differ significantly among treatments (29.8–30.8 Mg C ha^{-1}; $P > 0.05$). MAOC accounted for 99.9% and 96.4% of the SOC stock differences between *PO* and *PM* and between *PS* and *PM*, respectively. The proportional response of

MAOC exceeded that of POC in both mixtures (Holm-adjusted $P \leq 0.001$; Fig. 2e, f).

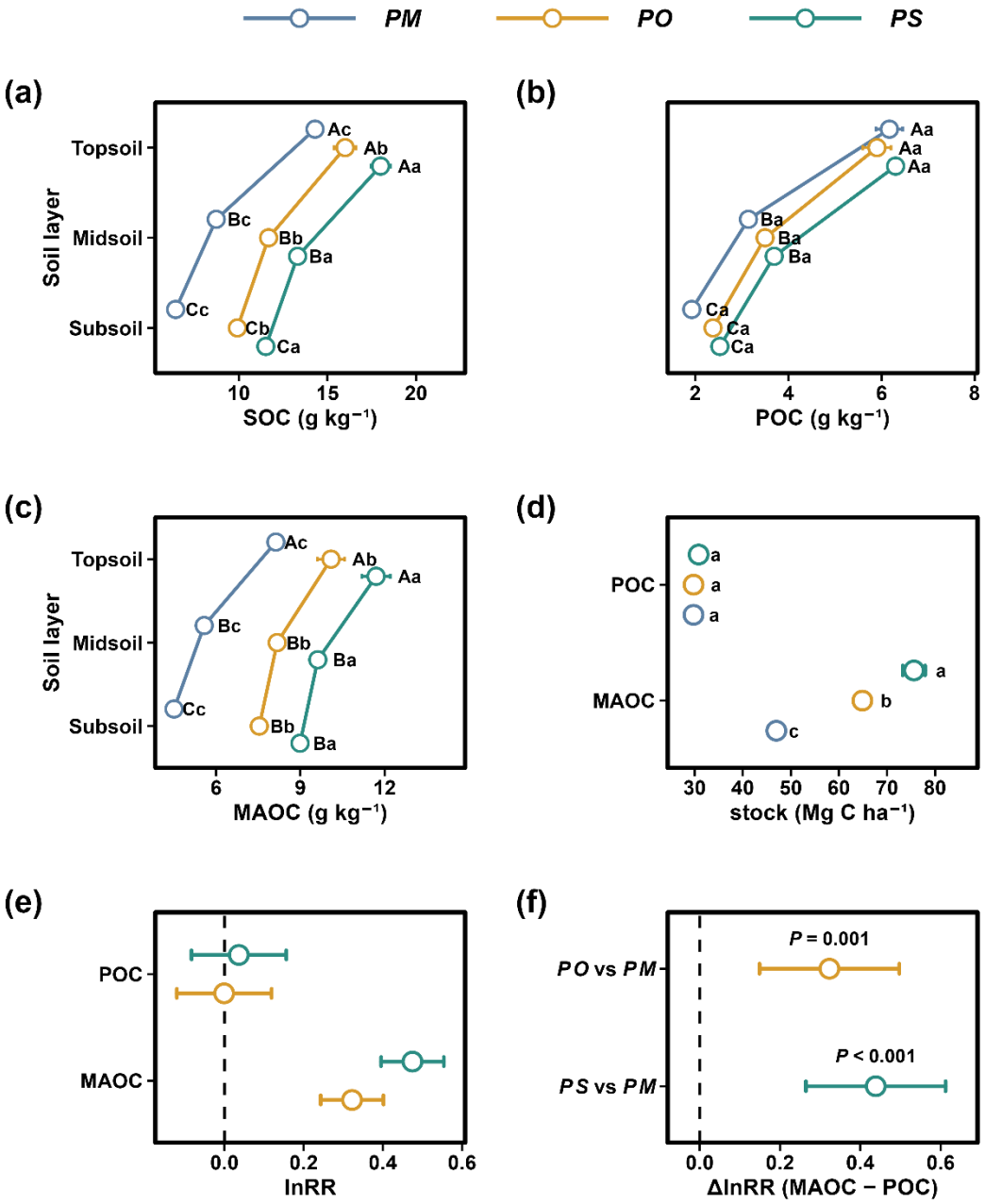

Fig. 2 Soil organic carbon fractions across soil layers and their 0–60 cm ESM stocks under the three planting treatments. Concentrations of (a) SOC, (b) POC, and (c) MAOC across topsoil, midsoil, and subsoil; (d) 0–60 cm stocks of POC and MAOC; (e) lnRR of POC and MAOC stocks in *PO* and *PS* relative to *PM*; and (f) differences between MAOC and POC lnRRs. Values in (a–d) are means ± SE. Different uppercase letters in (a–c) indicate significant differences among soil layers within a planting treatment, whereas different lowercase letters indicate significant differences

among planting treatments within a soil layer ($P < 0.05$). Different lowercase letters in (d) indicate significant differences among planting treatments within each carbon fraction ($P < 0.05$). Points and horizontal lines in (e,f) represent estimates and 95% confidence intervals, respectively. ESM, equivalent soil mass; SOC, soil organic carbon; POC, particulate organic carbon; MAOC, mineral-associated organic carbon; lnRR, log response ratio. Refer to Fig. 1 for treatment details.

3.3 *PO* and *PS* had higher soil nutrient availability, microbial biomass, and enzyme activities

Soil nutrient availability, microbial biomass, and potential enzyme activities were higher in *PO* and *PS* than in *PM* across all three soil layers (Fig. 3). Relative to *PM*, *PO* and *PS* had 36.9–55.0% higher AN and 59.3–86.1% higher AP. MBC was 34.4–47.9% higher in *PO* and 46.9–66.2% higher in *PS*; both treatments also had higher MBN and MBP. BG, NAG, ACP, and PER activities were 26.6–48.2% higher in *PO* and 43.6–70.5% higher in *PS*.

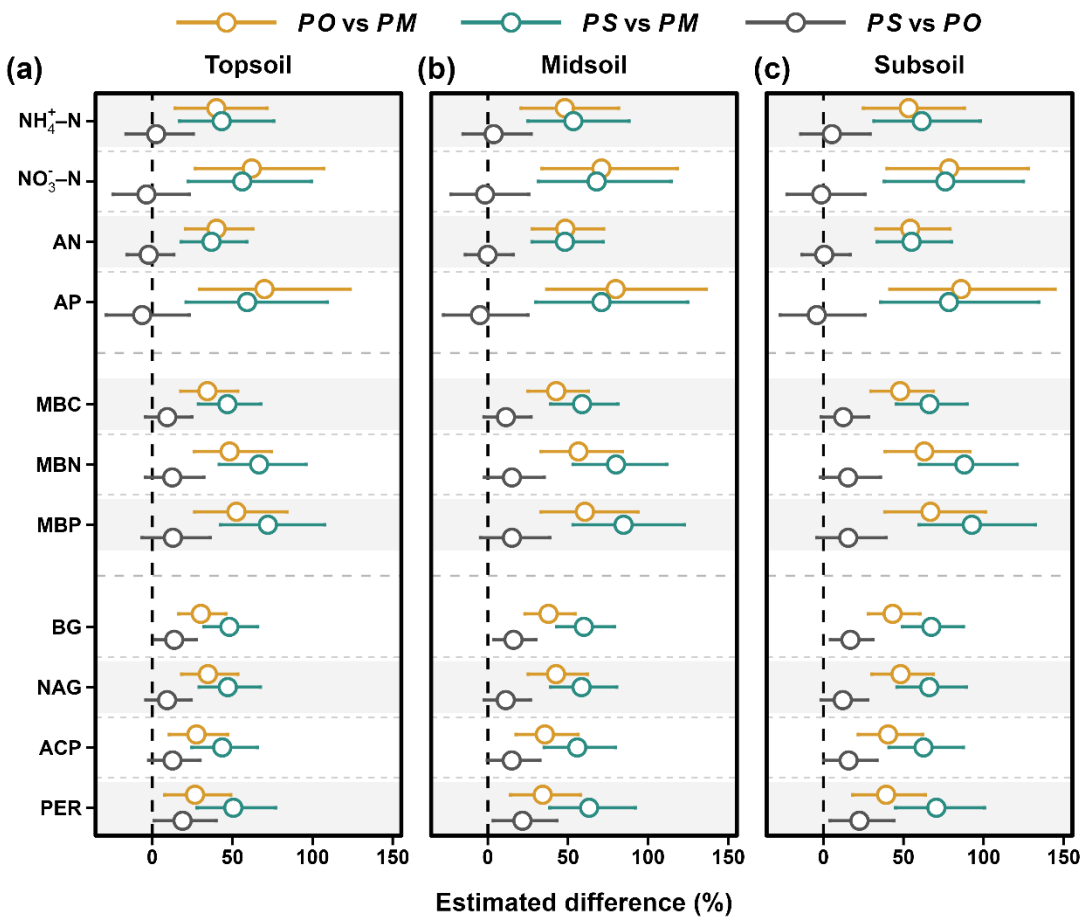

Fig. 3 Pairwise treatment differences in soil resource availability, microbial biomass, and potential extracellular enzyme activities across soil layers. (a) Topsoil; (b) midsoil; (c) subsoil. Points and horizontal lines represent estimated percentage differences and 95% confidence intervals, respectively. NH_4^+-N, ammonium N; NO_3^--N, nitrate N; AN, alkali-hydrolysable N; AP, available P; MBC, microbial biomass carbon; MBN, microbial biomass nitrogen; MBP, microbial biomass phosphorus; BG, β-1,4-glucosidase; NAG, β-1,4-N-acetylglucosaminidase; ACP, acid phosphatase; PER, peroxidase. Refer to Fig. 1 for treatment details.

3.4 Planting treatments differed in topsoil fungal composition

Topsoil fungal community composition differed among treatments (PERMANOVA: $R^2 = 0.563$, $P = 0.004$; Fig. 4a), whereas multivariate dispersion was similar among treatments (PERMDISP: $P = 0.207$). Fungal and bacterial alpha diversity did not differ among treatments (Shannon, Simpson, Chao1, or ACE indices; Table S5). *PO* had the highest predicted saprotroph proportion (59.7%) and the lowest pathotroph

proportion (12.5%), whereas *PS* had the highest symbiotroph proportion (38.8%; Fig. 4b). Among the selected ECM genera, *PO* had the highest mean relative abundances of *Russula* and *Tomentella*, whereas *PM* had the highest mean relative abundances of *Amanita* and *Hydnellum* (Fig. 4c).

(a)

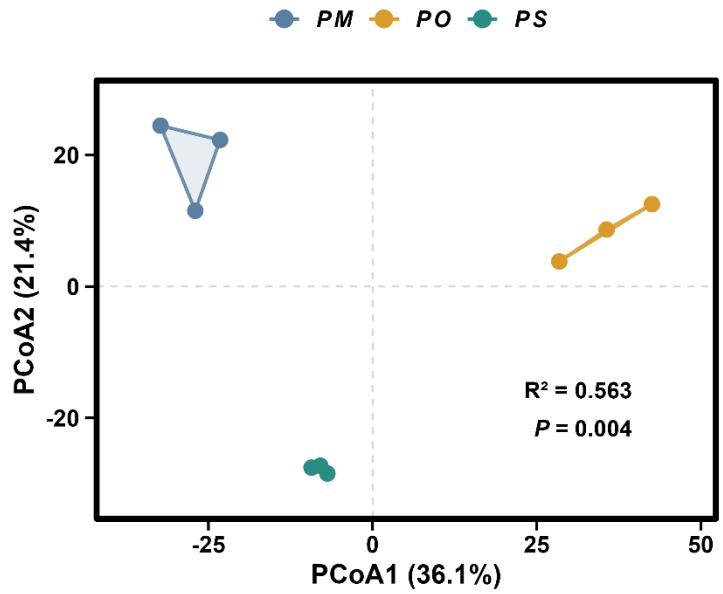
PM
PO
PS
20
0
-20
PCoA2 (21.4%)
R² = 0.563
P = 0.004
-25
0
25
50
PCoA1 (36.1%)

(b)

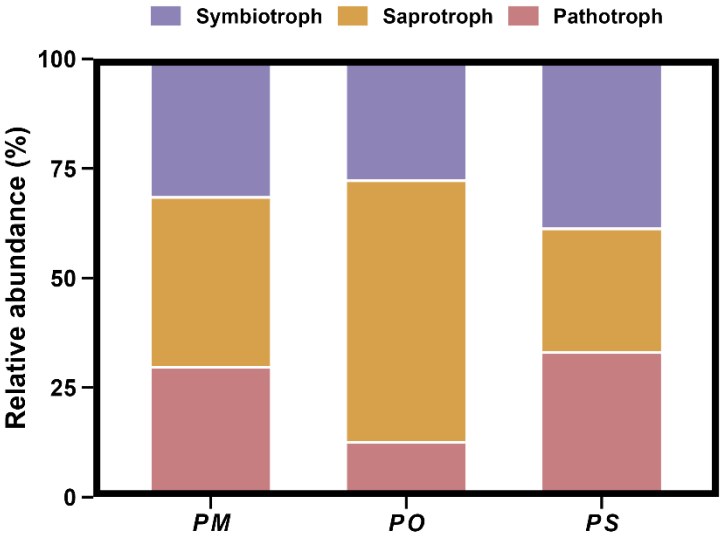
Symbiotroph
Saprotroph
Pathotroph
100
75
50
25
0
Relative abundance (%)
PM
PO
PS

(c)

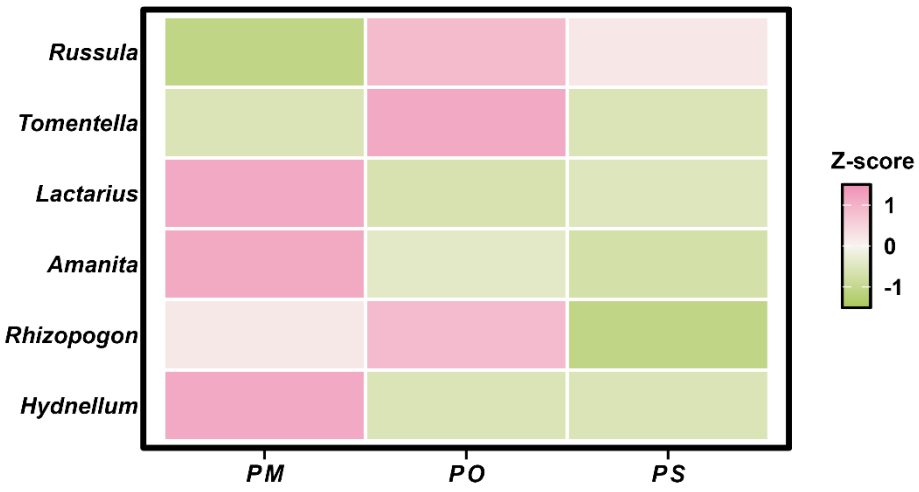
Russula
Tomentella
Lactarius
Amanita
Rhizopogon
Hydnellum
PM
PO
PS
Z-score
1
0
-1

Fig. 4 Topsoil fungal community composition and trophic structure under the three planting treatments. (a) Aitchison principal coordinates analysis (PCoA) of fungal community composition; (b) relative abundances of predicted fungal trophic modes; and (c) within-genus Z-scores of treatment-mean relative abundances of selected ectomycorrhizal (ECM) fungal genera. In (a), points represent plot-level samples, and lines and shaded polygons indicate treatment-specific convex hulls for visualization. Refer to Fig. 1 for treatment details.

3.5 MBC was more strongly associated with MAOC than with POC

MBC was positively associated with MAOC but showed little association with POC (Fig. 5). The MAOC slope exceeded the POC slope after FDR correction (q = 0.009). In contrast, AN, AP, BG, and PER showed no significant differences between the two C fractions (q = 0.349–0.516).

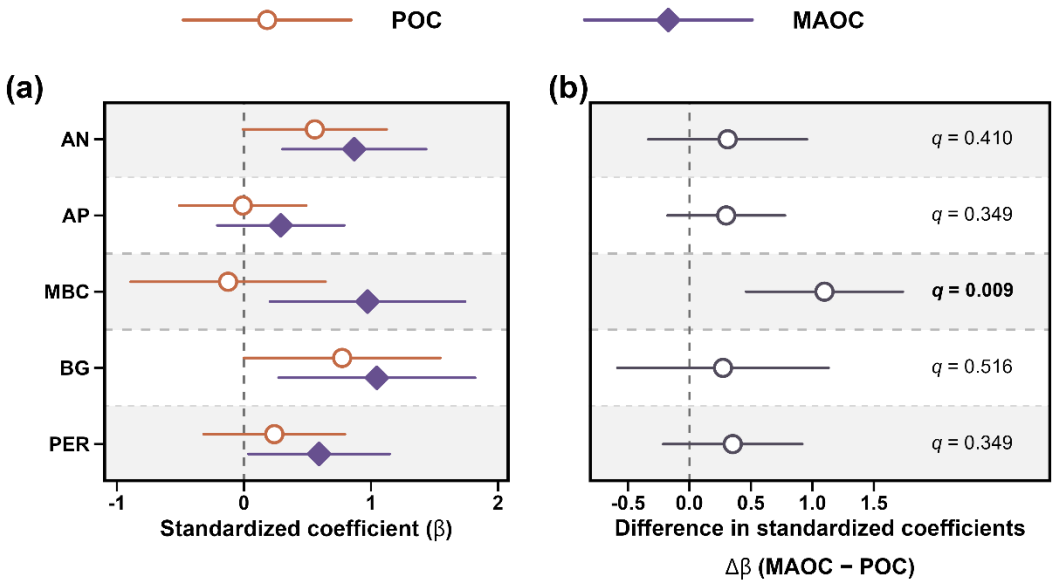

Fig. 5 Associations of soil resources and microbial attributes with POC and MAOC. (a) Standardized associations with POC and MAOC; and (b) differences between the corresponding MAOC and POC coefficients. Points and horizontal lines represent standardized slopes and 95% confidence intervals, respectively, and dashed vertical lines indicate zero. Positive values in (b) indicate stronger associations with MAOC than with POC. q values are FDR-adjusted P values for differences between fractions. POC, particulate organic carbon; MAOC, mineral-associated organic carbon. Refer to

Fig. 3 for abbreviations.

4 Discussion

4.1 *PS* stored more C in broadleaf trees and soil than *PO*

Eleven years after broadleaf underplanting, both mixed stands stored more ecosystem C than *PM* (Fig. 1). Retained pines accounted for most of the difference in live tree C stocks between the mixed stands and *PM* (Table S2). Higher C storage in the mixed stands agrees with evidence linking tree diversity to forest biomass and soil C accumulation (Arasa-Gisbert et al., 2018; Feng et al., 2022; Chen et al., 2023). Both mixtures had higher soil N and P availability than *PM* (Fig. 3), consistent with nutrient enrichment reported across *P. massoniana* mixtures (Yang et al., 2025). The relative contributions of retained pines and companion trees may change as the stands develop, because growth responses to mixing vary with stand density and development (Mina et al., 2018; Bertrand and Morin, 2026).

PO and *PS* received companion seedlings at the same initial density, but *PS* stored 4.8 times as much C in broadleaf trees as *PO* (Table S2). Neither retained pine C nor total live tree C differed significantly between the mixtures. Differences in crown development and resource acquisition can produce unequal growth responses among component species (Forrester and Bauhus, 2016; Jensen et al., 2025). Greater canopy structural complexity can strengthen complementarity among tree species (Deng et al., 2025), while competition can constrain the growth of individual species. For example, introducing *Phoebe zhennan* into *Cunninghamia lanceolata* plantations increased resource use efficiency and stand gross primary productivity while reducing

growth of the retained conifer (Liu et al., 2024). The contrasting broadleaf C stocks in *PO* and *PS* therefore suggest that companion species identity matters for the contributions of individual tree species to stand C storage, even at the same species richness (Wu et al., 2025).

PS stored more SOC than *PO* despite its smaller understory and forest floor litter C pools (Fig. 1; Table S2). Standing litter stocks reflect the balance between litter supply and decomposition, whereas SOC stocks integrate plant inputs, microbial transformation, and physicochemical retention (Augusto and Boča, 2022). Companion species can also alter the quantity and quality of C entering soil through roots and rhizodeposition. In experimental *P. massoniana* mixtures, SOC chemistry covaried with litter and fine root traits, with closer relationships for roots than litter (Wang et al., 2019). Across European forests, tree species mixing influenced microbial functioning indirectly through changes in litter and root traits and soil properties (Gillespie et al., 2021). Evidence from degraded *P. massoniana* forests also links SOC gains under species mixing to greater plant inputs and microbial residue accumulation (Tang et al., 2025). Mixing can also stimulate SOC mineralization in conifer rhizospheres (Li et al., 2022). The higher SOC stock in *PS* may therefore reflect differences in belowground C inputs, microbial processing, and retention that are not captured by forest floor litter C stocks.

4.2 Higher SOC stocks chiefly reflected greater MAOC stocks

MAOC accounted for most of the SOC stock differences among treatments. Both mixed stands stored more MAOC than *PM*, and *PS* stored more MAOC than *PO*,

whereas POC stocks did not differ significantly among treatments (Fig. 2d). The direct comparison of fraction responses also identified a greater proportional response of MAOC than POC in both mixed stands (Fig. 2e, f).

POC and MAOC can contribute differently to higher SOC stocks in mixed stands. Mixed plantations commonly store more SOC than pure plantations, although the response varies with establishment history and site conditions (Yu et al., 2023; Li et al., 2025). A recent global synthesis found that mixed forestation increased both POC and MAOC (Shu et al., 2026). Natural secondary forests also contained more coarse and fine particulate C than adjacent *P. massoniana* plantations (Yuan et al., 2022). Similar POC stocks may reflect different balances among C inputs, decomposition, and transformation. Plant fragments enter POC, while decomposition releases compounds that microorganisms can assimilate or that can interact directly with minerals. The microbial efficiency–matrix stabilization framework links the processing of plant substrates to the formation of persistent organic matter (Cotrufo et al., 2013). Tracer experiments further distinguish biochemical and physical pathways through which litter contributes to soil organic matter (Cotrufo et al., 2015). Decomposing particulate material can itself provide surfaces where microbial products, minerals, and aggregates accumulate (Witzgall et al., 2021). Particulate material can therefore supply C for MAOC formation without accumulating as a larger POC stock (Cotrufo et al., 2019; Lavallee et al., 2020).

Mineral interactions help determine how much of the supplied C remains in soil. Organic matter persistence depends on its accessibility to decomposers and its

environment, rather than chemical resistance alone (Lehmann and Kleber, 2015). Work in *P. massoniana* mixtures links Fe oxides to C retention within soil aggregates (Han et al., 2024). Mineral properties and existing C loads also help determine how much additional MAOC a soil can retain (Georgiou et al., 2022). However, mineral surfaces can both retain organic compounds and participate in reactions that transform or release them (Kleber et al., 2021). The larger MAOC stock in *PS* could partly reflect differences in mineral interactions. Because MAOC was calculated as SOC minus POC, a larger stock alone does not establish a longer C residence time. MAOC concentrations were higher in both mixed stands across all three soil layers, with the largest proportional differences relative to *PM* at 40–60 cm (Fig. 2c). Roots supply C directly to deeper soil, while dissolved organic matter transports C from shallower horizons (Rumpel and Kögel-Knabner, 2011). Microcosm experiments found that belowground delivery favored microbial formation of MAOC (Sokol and Bradford, 2019), and forest tracer studies identified substantial root derived inputs to mineral-associated pools (Keller et al., 2021). Sampling only the topsoil would therefore miss part of the MAOC difference among treatments.

4.3 MBC was more strongly associated with MAOC than with POC

MBC was positively associated with MAOC after accounting for treatment and soil layer, whereas its association with POC was weak (Fig. 5). The difference between these slopes remained significant after correction for multiple comparisons (q = 0.009). AN, AP, BG, and PER did not have significantly different slopes for the two fractions. Microbial growth and turnover provide a plausible explanation for the

stronger association between MBC and MAOC. Microorganisms assimilate plant compounds, build cells, and release products during growth and death. Experiments demonstrate that microbial products can form persistent soil organic matter (Kallenbach et al., 2016), while the microbial C pump framework emphasizes the contribution of biomass production to soil C storage (Liang et al., 2017). Microbial residues subsequently accumulate or are recycled, depending on their properties, microbial activity, and interactions with the soil matrix (Liang et al., 2019; Buckeridge et al., 2022; Sokol et al., 2022). Both mixed stands had higher MBC than *PM* across the sampled layers (Fig. 3). Soil nutrient availability can support microbial growth and influence both POC and MAOC. Both mixed stands contained more alkali-hydrolysable N and available P than *PM* (Fig. 3). Experiments mixing *Eucalyptus urophylla* with N fixing *Acacia mangium* likewise linked changes in nutrient and litter conditions to greater microbial biomass (Huang et al., 2014). Nutrient supply can change the balance between microbial growth and respiration, but this balance also depends on substrate stoichiometry and environmental conditions (Manzoni et al., 2012). AN and AP reflect nutrient release, uptake, and recycling. Their associations with POC and MAOC may therefore integrate several processes, consistent with the absence of a clear difference between their slopes for the two fractions.

Potential enzyme activities indicate the capacity to break down substrates; SOC retention also depends on how microorganisms use the released C. Both mixed stands had higher BG, NAG, ACP, and PER activities than *PM* (Fig. 3). Related work in

mixed *Eucalyptus* plantations linked microbial communities and enzyme activities to changes in SOC chemistry (Huang et al., 2017). Extracellular breakdown supplies compounds for both microbial growth and respiration. Global analyses link microbial C use efficiency—the fraction of acquired C used for growth—to SOC storage (Tao et al., 2023). Extracellular enzymes regulate substrate depolymerization rather than the subsequent fate of assimilated C. In our models, neither BG nor PER showed a significantly stronger association with MAOC than with POC (Fig. 5). Topsoil fungal composition differed among treatments, whereas fungal alpha diversity did not differ significantly (Fig. 4a; Table S5). *PO* had the highest mean proportion of predicted saprotrophs (59.7%), whereas *PS* had the highest mean proportion of predicted symbiotrophs (38.8%; Fig. 4b). These differences may reflect variation in litter substrates and root environments among companion species. Mycorrhizal associations can modify the productivity of tree mixtures (Luo et al., 2024), and fungal hyphae transfer plant derived C into soil and influence its transformation (Frey, 2019). Fungal contributions to soil C depend on C delivery and turnover as well as community composition. Despite the higher mean proportion of predicted symbiotrophs in *PS*, selected ectomycorrhizal genera, including *Russula* and *Tomentella*, had their highest mean relative abundances in *PO* (Fig. 4c). Their relative abundances therefore did not follow the MAOC ranking. In temperate forest tracer studies, arbuscular mycorrhizal stands received more root derived C in mineral-associated pools than ectomycorrhizal stands (Keller et al., 2021). These patterns suggest that the observed fungal

community differences were not consistently aligned with MAOC stocks among treatments.

Repeated inventories could establish whether the larger broadleaf C pool and higher SOC stock in *PS* persist as retained pines and companion trees develop. Combining root derived C tracing with measurements of microbial residues and mineral properties could distinguish C delivery, microbial transformation, and retention.

5 Conclusion

Eleven years after broadleaf underplanting, both mixed stands stored more ecosystem C than pure *P. massoniana* stands. Retained pines accounted for most of the larger live tree C stocks in the mixed stands relative to the pure stands. *PS* stored more ecosystem C, SOC, and broadleaf tree C than *PO*, although total live tree C did not differ significantly between the two mixed stands. Higher SOC stocks chiefly reflected greater MAOC stocks, and differences in MAOC concentrations extended to the 40–60 cm layer. Microbial biomass C was more strongly associated with MAOC than with POC. These findings support evaluating companion species using ecosystem C stocks, with particular attention to companion-tree C and soil MAOC rather than total live-tree C alone.

CRediT authorship contribution statement

Zeyao Zhao: Writing – original draft, Writing – review & editing, Methodology, Formal analysis, Data curation, Conceptualization. Nan Jiang: Investigation, Formal analysis, Data curation. Wenjun Xie: Methodology, Investigation. Kangwei Zhao: Investigation, Formal analysis. Jieyu Zhang: Formal analysis, Data curation. Miaoyan

Quan: Investigation, Methodology. Zhaogui Yan: Writing – review & editing, Visualization, Validation, Supervision, Resources. Li Mei: Writing – review & editing, Validation, Supervision, Resources, Project administration, Methodology, Funding acquisition, Conceptualization.

Declaration of competing interests

In submitting this manuscript, we provide the following statements: (1) No conflict of interest exists in the submission of this manuscript; (2) The manuscript is approved by all authors; (3) The work described was original and has not been published previously, and is not under consideration for publication elsewhere; (4) All the authors listed have made substantial contributions to the research design, or the acquisition, analysis or interpretation of data, or drafting the paper or revising it critically; and (5) Nobody who qualifies for authorship has been excluded.

Acknowledgements

This study was supported by National Key Research and Development Program of China (Grant Nos. 2023YFD2200902 and 2023YFD2200401). We thank the members of the Hubei Engineering Technology Research Center for Forestry Information Laboratory for their invaluable assistance.

Data availability

Data will be made available on request.

References

Arasa-Gisbert, R., Vayreda, J., Román-Cuesta, R.M., Villela, S.A., Mayorga, R., Retana, J., 2018. Forest diversity plays a key role in determining the stand

548 carbon stocks of Mexican forests. Forest Ecology and Management 415-416,
549 160–171. https://doi.org/10.1016/j.foreco.2018.02.023.
550 Augusto, L., Boča, A., 2022. Tree functional traits, forest biomass, and tree species
551 diversity interact with site properties to drive forest soil carbon. Nature
552 Communications 13, 1097. https://doi.org/10.1038/s41467-022-28748-0.
553 Bao, S.D., 2000. Soil and Agricultural Chemistry Analysis, third ed. China
554 Agriculture Press, Beijing (in Chinese).
555 Bertrand, R., Morin, X., 2026. Biodiversity insurance of forest productivity has
556 strengthened under recent climate change. Global Change Biology 32, e70760.
557 https://doi.org/10.1111/gcb.70760.
558 Buckeridge, K.M., Creamer, C., Whitaker, J., 2022. Deconstructing the microbial
559 necromass continuum to inform soil carbon sequestration. Functional Ecology
560 36, 1396–1410. https://doi.org/10.1111/1365-2435.14014.
561 Chen, X., Taylor, A.R., Reich, P.B., Hisano, M., Chen, H.Y.H., Chang, S.X., 2023.
562 Tree diversity increases decadal forest soil carbon and nitrogen accrual. Nature
563 618, 94–101. https://doi.org/10.1038/s41586-023-05941-9.
564 Cotrufo, M.F., Ranalli, M.G., Haddix, M.L., Six, J., Lugato, E., 2019. Soil carbon
565 storage informed by particulate and mineral-associated organic matter. Nature
566 Geoscience 12, 989–994. https://doi.org/10.1038/s41561-019-0484-6.
567 Cotrufo, M.F., Soong, J.L., Horton, A.J., Campbell, E.E., Haddix, M.L., Wall, D.H.,
568 Parton, W.J., 2015. Formation of soil organic matter via biochemical and
569 physical pathways of litter mass loss. Nature Geoscience 8, 776–779.

https://doi.org/10.1038/ngeo2520.

Cotrufo, M.F., Wallenstein, M.D., Boot, C.M., Denef, K., Paul, E., 2013. The Microbial Efficiency–Matrix Stabilization (MEMS) framework integrates plant litter decomposition with soil organic matter stabilization: do labile plant inputs form stable soil organic matter? Global Change Biology 19, 988–995. https://doi.org/10.1111/gcb.12113.

Deng, X., Schmid, B., Bruelheide, H., Chen, C., Li, Y., Li, S., Morsdorf, F., Ray, T., Schuman, M.C., Tang, T., von Oheimb, G., Ma, K., Liu, X., 2025. Forest biodiversity increases productivity via complementarity from greater canopy structural complexity. Proceedings of the National Academy of Sciences 122, e2506750122. https://doi.org/10.1073/pnas.2506750122.

Feng, Y., Schmid, B., Loreau, M., Forrester, D.I., Fei, S., Zhu, J., Tang, Z., Zhu, J., Hong, P., Ji, C., Shi, Y., Su, H., Xiong, X., Xiao, J., Wang, S., Fang, J., 2022. Multispecies forest plantations outyield monocultures across a broad range of conditions. Science 376, 865–868. https://doi.org/10.1126/science.abm6363.

Forrester, D.I., Bauhus, J., 2016. A review of processes behind diversity–productivity relationships in forests. Current Forestry Reports 2, 45–61. https://doi.org/10.1007/s40725-016-0031-2.

Frey, S.D., 2019. Mycorrhizal fungi as mediators of soil organic matter dynamics. Annual Review of Ecology, Evolution, and Systematics 50, 237–259. https://doi.org/10.1146/annurev-ecolsys-110617-062331.

Georgiou, K., Jackson, R.B., Vindušková, O., Abramoff, R.Z., Ahlström, A., Feng, W.,

592 Harden, J.W., Pellegrini, A.F.A., Polley, H.W., Soong, J.L., Riley, W.J., Torn,
593 M.S., 2022. Global stocks and capacity of mineral-associated soil organic
594 carbon. Nature Communications 13, 3797. https://doi.org/10.1038/s41467-
595 022-31540-9.
596 Gillespie, L.M., Hättenschwiler, S., Milcu, A., Wambsganss, J., Shihan, A., Fromin,
597 N., 2021. Tree species mixing affects soil microbial functioning indirectly via
598 root and litter traits and soil parameters in European forests. Functional
599 Ecology 35, 2190–2204. https://doi.org/10.1111/1365-2435.13877.
600 Han, Z., Zhou, Y., Guo, Y., Liu, H., Sun, B., 2024. Organic carbon sequestration by Fe
601 oxides in aggregates in a *Pinus massoniana* conifer-broadleaf mixed forest.
602 Soil and Tillage Research 240, 106105.
603 https://doi.org/10.1016/j.still.2024.106105.
604 Huang, Q., Wang, B., Shen, J., Xu, F., Li, N., Jia, P., Jia, Y., An, S., Amoah, I.D.,
605 Huang, Y., 2024. Shifts in C-degradation genes and microbial metabolic
606 activity with vegetation types affected the surface soil organic carbon pool.
607 Soil Biology and Biochemistry 192, 109371.
608 https://doi.org/10.1016/j.soilbio.2024.109371.
609 Huang, X., Liu, S., Wang, H., Hu, Z., Li, Z., You, Y., 2014. Changes of soil microbial
610 biomass carbon and community composition through mixing nitrogen-fixing
611 species with *Eucalyptus urophylla* in subtropical China. Soil Biology and
612 Biochemistry 73, 42–48. https://doi.org/10.1016/j.soilbio.2014.01.021.
613 Huang, X., Liu, S., You, Y., Wen, Y., Wang, H., Wang, J., 2017. Microbial community

and associated enzymes activity influence soil carbon chemical composition in *Eucalyptus urophylla* plantation with mixing N_2-fixing species in subtropical China. Plant and Soil 414, 199–212. https://doi.org/10.1007/s11104-016-3117-5.

Jensen, J., Blondeel, H., Guillemot, J., Schnabel, F., Serrano-León, H., Auge, H., Baeten, L., Barsoum, N., Bauhus, J., Baum, C., Bermudez, R., Beyer, F., Brancalion, P., Cavender-Bares, J., Eisenhauer, N., Felton, A., Ferlian, O., Fiedler, S., Gebauer, T., Godbold, D.L., Hajek, P., Hall, J.S., Hölscher, D., Jactel, H., Kreft, H., Lapadat, C., MacLaren, C., Martin-StPaul, N., Meredieu, C., Mereu, S., Messier, C., Montgomery, R.A., Muys, B., Nock, C.A., Parker, J.D., Parker, W.C., Paterno, G.B., Perring, M.P., Ponette, Q., Potvin, C., Reich, P.B., Rentch, J., Rewald, B., Robin, A., Scherer-Lorenzen, M., Sandén, H., Sinacore, K., Standish, R.J., Stefanski, A., Verheyen, K., Williams, L.J., Weih, M., 2025. Diversity in resource use strategies promotes productivity in young planted tree species mixtures. Global Change Biology 31, e70493. https://doi.org/10.1111/gcb.70493.

Jia, L., Jiang, Q., Sun, J., Robinson, D., Yang, Z., Yao, X., Wang, X., Dai, X., Chen, T., Wu, D., Fan, A., Yang, L., Chen, G., Yang, Y., 2024. Contrasting depth-related fine root plastic responses to soil warming in a subtropical Chinese fir plantation. Journal of Ecology 112, 1058–1073. https://doi.org/10.1111/1365-2745.14286.

Joshi, R.K., Garkoti, S.C., 2023. Influence of vegetation types on soil physical and

636 chemical properties, microbial biomass and stoichiometry in the central
637 Himalaya. CATENA 222, 106835.
638 https://doi.org/10.1016/j.catena.2022.106835.
639 Kallenbach, C.M., Frey, S.D., Grandy, A.S., 2016. Direct evidence for microbial-
640 derived soil organic matter formation and its ecophysiological controls. Nature
641 Communications 7, 13630. https://doi.org/10.1038/ncomms13630.
642 Keller, A.B., Brzostek, E.R., Craig, M.E., Fisher, J.B., Phillips, R.P., 2021. Root-
643 derived inputs are major contributors to soil carbon in temperate forests, but
644 vary by mycorrhizal type. Ecology Letters 24, 626–635.
645 https://doi.org/10.1111/ele.13651.
646 Kleber, M., Bourg, I.C., Coward, E.K., Hansel, C.M., Myneni, S.C.B., Nunan, N.,
647 2021. Dynamic interactions at the mineral–organic matter interface. Nature
648 Reviews Earth & Environment 2, 402–421. https://doi.org/10.1038/s43017-
649 021-00162-y.
650 Lavallee, J.M., Soong, J.L., Cotrufo, M.F., 2020. Conceptualizing soil organic matter
651 into particulate and mineral-associated forms to address global change in the
652 21st century. Global Change Biology 26, 261–273.
653 https://doi.org/10.1111/gcb.14859.
654 Lehmann, J., Kleber, M., 2015. The contentious nature of soil organic matter. Nature
655 528, 60–68. https://doi.org/10.1038/nature16069.
656 Li, M., Ding, X., Chen, M., Zhang, X., Zhao, Y., Meng, M., Zhang, G., Cao, Y., 2025.
657 Mixed plantations enhance soil aggregation and carbon storage: A global

meta-analysis. Catena 254, 109013.
https://doi.org/10.1016/j.catena.2025.109013.
Li, W.Q., Wu, Z.J., Zong, Y.Y., Wang, G.G., Chen, F.S., Liu, Y.Q., Li, J.J., Fang, X.M., 2022. Tree species mixing enhances rhizosphere soil organic carbon mineralization of conifers in subtropical plantations. Forest Ecology and Management 516, 120238. https://doi.org/10.1016/j.foreco.2022.120238.
Liang, C., Amelung, W., Lehmann, J., Kästner, M., 2019. Quantitative assessment of microbial necromass contribution to soil organic matter. Global Change Biology 25, 3578–3590. https://doi.org/10.1111/gcb.14781.
Liang, C., Schimel, J.P., Jastrow, J.D., 2017. The importance of anabolism in microbial control over soil carbon storage. Nature Microbiology 2, 17105. https://doi.org/10.1038/nmicrobiol.2017.105.
Liu, Z., Wang, X., Jia, G., Jiang, J., Liao, B., 2024. Introduction of broadleaf tree species can promote the resource use efficiency and gross primary productivity of pure forests. Plant, Cell & Environment 47, 5252–5264. https://doi.org/10.1111/pce.15096.
Luo, S., Schmid, B., Hector, A., Scherer-Lorenzen, M., Verheyen, K., Barsoum, N., Bauhus, J., Beyer, F., Bruelheide, H., Ferlian, O., Godbold, D., Hall, J.S., Hajek, P., Huang, Y., Hölscher, D., Kreft, H., Liu, X., Messier, C., Nock, C., Paquette, A., Parker, J.D., Parker, W.C., Paterno, G.B., Reich, P.B., Rewald, B., Sandén, H., Sinacore, K., Stefanski, A., Williams, L., Eisenhauer, N., 2024. Mycorrhizal associations modify tree diversity−productivity relationships

across experimental tree plantations. New Phytologist 243, 1205–1219. https://doi.org/10.1111/nph.19889.

Luo, Y.J., Wang, X.K., Ouyang, Z.Y., Lu, F., Feng, L.G., Tao, J., 2020. A review of biomass equations for China's tree species. Earth System Science Data 12, 21–40. https://doi.org/10.5194/essd-12-21-2020.

Manzoni, S., Taylor, P., Richter, A., Porporato, A., Ågren, G.I., 2012. Environmental and stoichiometric controls on microbial carbon-use efficiency in soils. New Phytologist 196, 79–91. https://doi.org/10.1111/j.1469-8137.2012.04225.x.

Mina, M., Huber, M.O., Forrester, D.I., Thürig, E., Rohner, B., 2018. Multiple factors modulate tree growth complementarity in Central European mixed forests. Journal of Ecology 106, 1106–1119. https://doi.org/10.1111/1365-2745.12846.

Nguyen, N.H., Song, Z., Bates, S.T., Branco, S., Tedersoo, L., Menke, J., Schilling, J.S., Kennedy, P.G., 2016. FUNGuild: An open annotation tool for parsing fungal community datasets by ecological guild. Fungal Ecology 20, 241–248. https://doi.org/10.1016/j.funeco.2015.06.006.

Pan, Y., Birdsey, R.A., Phillips, O.L., Houghton, R.A., Fang, J., Kauppi, P.E., Keith, H., Kurz, W.A., Ito, A., Lewis, S.L., Nabuurs, G.J., Shvidenko, A., Hashimoto, S., Lerink, B., Schepaschenko, D., Castanho, A., Murdiyarso, D., 2024. The enduring world forest carbon sink. Nature 631, 563–569. https://doi.org/10.1038/s41586-024-07602-x.

Qi, D., Feng, F., Lu, C., Fu, Y., 2022. C:N:P stoichiometry of different soil components after the transition of temperate primary coniferous and broad-

leaved mixed forests to secondary forests. Soil and Tillage Research 216, 105260. https://doi.org/10.1016/j.still.2021.105260.

R Core Team, 2024. R: A Language and Environment for Statistical Computing. R Foundation for Statistical Computing, Vienna, Austria. https://www.R-project.org/.

Rumpel, C., Kögel-Knabner, I., 2011. Deep soil organic matter—a key but poorly understood component of terrestrial C cycle. Plant and Soil 338, 143–158. https://doi.org/10.1007/s11104-010-0391-5.

Schnabel, F., Guillemot, J., Barry, K.E., Brunn, M., Cesarz, S., Eisenhauer, N., Gebauer, T., Guerrero-Ramirez, N.R., Handa, I.T., Madsen, C., Mancilla, L., Monteza, J., Moore, T., Oelmann, Y., Scherer-Lorenzen, M., Schwendenmann, L., Wagner, A., Wirth, C., Potvin, C., 2025. Tree diversity increases carbon stocks and fluxes above—but not belowground in a tropical forest experiment. Global Change Biology 31, e70089. https://doi.org/10.1111/gcb.70089.

Shu, X., Chen, D., Chen, J., Zhou, Z., Luo, Y., Zhang, Y., Tang, H., Deng, D., Xia, L., 2026. Mixed forestation outperforms pure stands in soil carbon sequestration and stability. Global Change Biology 32, e70812. https://doi.org/10.1111/gcb.70812.

Sokol, N.W., Bradford, M.A., 2019. Microbial formation of stable soil carbon is more efficient from belowground than aboveground input. Nature Geoscience 12, 46–53. https://doi.org/10.1038/s41561-018-0258-6.

Sokol, N.W., Slessarev, E., Marschmann, G.L., Nicolas, A., Blazewicz, S.J., Brodie,

E.L., Firestone, M.K., Foley, M.M., Hestrin, R., Hungate, B.A., Koch, B.J., Stone, B.W., Sullivan, M.B., Zablocki, O., LLNL Soil Microbiome Consortium, Trubl, G., McFarlane, K., Stuart, R., Nuccio, E., Weber, P., Jiao, Y., Zavarin, M., Kimbrel, J., Morrison, K., Adhikari, D., Bhattacharaya, A., Nico, P., Tang, J., Didonato, N., Paša-Tolić, L., Greenlon, A., Sieradzki, E.T., Dijkstra, P., Schwartz, E., Sachdeva, R., Banfield, J., Pett-Ridge, J., 2022. Life and death in the soil microbiome: how ecological processes influence biogeochemistry. Nature Reviews Microbiology 20, 415–430. https://doi.org/10.1038/s41579-022-00695-z.

Tang, F., Zhou, Y., Feng, J., Li, J., Feng, J., Lv, Y., Mao, Y., Wang, Y., Deng, P., Bai, Y., 2025. Important role of *Pinus massoniana* mixed forests in enhancing soil carbon stocks in degraded forests in southern China. CATENA 250, 108792. https://doi.org/10.1016/j.catena.2025.108792.

Tao, F., Huang, Y., Hungate, B.A., Manzoni, S., Frey, S.D., Schmidt, M.W.I., Reichstein, M., Carvalhais, N., Ciais, P., Jiang, L., Lehmann, J., Wang, Y.P., Houlton, B.Z., Ahrens, B., Mishra, U., Hugelius, G., Hocking, T.D., Lu, X., Shi, Z., Viatkin, K., Vargas, R., Yigini, Y., Omuto, C., Malik, A.A., Peralta, G., Cuevas-Corona, R., Di Paolo, L.E., Luotto, I., Liao, C., Liang, Y.S., Saynes, V.S., Huang, X., Luo, Y., 2023. Microbial carbon use efficiency promotes global soil carbon storage. Nature 618, 981–985. https://doi.org/10.1038/s41586-023-06042-3.

Ulbrich, T.C., Rivas-Ubach, A., Tiemann, L.K., Friesen, M.L., Evans, S.E., 2022.

Plant root exudates and rhizosphere bacterial communities shift with neighbor context. Soil Biology and Biochemistry 172, 108753. https://doi.org/10.1016/j.soilbio.2022.108753.

Wang, H., Liu, S., Song, Z., Yang, Y., Wang, J., You, Y., Zhang, X., Shi, Z., Nong, Y., Ming, A., Lu, L., Cai, D., 2019. Introducing nitrogen-fixing tree species and mixing with *Pinus massoniana* alters and evenly distributes various chemical compositions of soil organic carbon in a planted forest in southern China. Forest Ecology and Management 449, 117477. https://doi.org/10.1016/j.foreco.2019.117477.

Wendt, J.W., Hauser, S., 2013. An equivalent soil mass procedure for monitoring soil organic carbon in multiple soil layers. European Journal of Soil Science 64, 58–65. https://doi.org/10.1111/ejss.12002.

Witzgall, K., Vidal, A., Schubert, D.I., Höschen, C., Schweizer, S.A., Buegger, F., Pouteau, V., Chenu, C., Mueller, C.W., 2021. Particulate organic matter as a functional soil component for persistent soil organic carbon. Nature Communications 12, 4115. https://doi.org/10.1038/s41467-021-24192-8.

Wu, Y., Zheng, J., Gao, J., He, X., Liu, X., Chen, Y., Liu, J., Li, C., 2025. Functional diversity explains ecosystem carbon storage in subtropical forests. Global Change Biology 31, e70120. https://doi.org/10.1111/gcb.70120.

Yang, C., Jiang, P., Qian, Z., Sun, J., Wu, T., Yang, Z., Sun, Y., Huang, X., 2025. Evolutionary history of mixed tree species improved soil nutrient content of *Pinus massoniana* plantation. Plant and Soil 513, 1–16.

https://doi.org/10.1007/s11104-024-07197-2.

Yu, Z., Wang, K., Li, J., Shangguan, Z., Deng, L., 2023. Mixed plantations have more soil carbon sequestration benefits than pure plantations in China. Forest Ecology and Management 529, 120654. https://doi.org/10.1016/j.foreco.2022.120654.

Yu, Z., Zhang, W., He, H., Li, Y., Xie, Z., Sailike, A., Hao, H., Tian, X., Sun, L., Liang, Y., Fu, R., Yang, P., 2024. The CAZyme family regulates the changes in soil organic carbon composition during vegetation restoration in the Mu Us desert. Geoderma 452, 117109. https://doi.org/10.1016/j.geoderma.2024.117109.

Yuan, Z., Jin, X., Xiao, W., Wang, L., Sun, Y., Guan, Q., Meshack, A.O., 2022. Comparing soil organic carbon stock and fractions under natural secondary forest and *Pinus massoniana* plantation in subtropical China. CATENA 212, 106092. https://doi.org/10.1016/j.catena.2022.106092.

Supplementary Files

This is a list of supplementary files associated with this preprint. Click to download.

- Supplementary.docx
- Highlights.docx